Optimized Blood Pressure Classification by Features of Pulse Rate Variability and Asymmetry

Aikaterini Vraka[1], Vicente Bertomeu-González[2], Aurelio Quesada[3],
Roberto Zangróniz[4], Raúl Alcaraz[4], José J Rieta[1]

[1] BioMIT.org, Electronic Engineering Department, Universitat Politecnica de Valencia, Spain
[2] Department of Clinical Medicine, Miguel Hernandez University, Spain
[3] Cardiology Department, General University Hospital Consortium of Valencia,Spain
[4] Research Group in Electronic, Biomed. and Telecomm. Eng., Univ. of Castilla-La Mancha, Spain

Abstract

Pulse-rate variability (PRV) is a rather interesting alternative in blood pressure (BP) estimation. Notwithstanding, the suitability of PRV for BP monitoring is under dispute, while the performance of the reported PRV studies could be improved. Five-minute electrocardiography (ECG) and PPG recordings of 202 patients from the MIMIC-II database were recruited and classified into normotensive (NT), prehypertensive (PHT) and hypertensive (HT). PRV and asymmetry analysis was performed using time-, frequency-domain and non-linear indices. HRV was used to verify the results using Bland-Altman (BA) and correlation. Multi-class (MCC) and single-class classification was performed with 10*-fold cross-validation and a 20% test set. For all but NT group, correlation was high (*$\rho \geq 0.8$*,* $p < 0.05$*) for all features except for LF/HF. BA analysis suggests a high concordance between most PRV and HRV features (CI >* 90%*, BA ratio <* 10%*). MCC, NT and HT classification accuracy was up to* 95%*,* 90% *and* 92.5% *using 6-, 7- and 5-feature models, respectively. PRV is reliable in monitoring BP in critically-ill patients. Adding pulse-rate asymmetry to PRV analysis significantly improves the results and outperforms previous studies applying PRV for BP estimation using the same database.*

1. Introduction

Connected with premature morbidity, hypertension (HT) currently affects more than one billion people [1]. The most efficient way to face HT and its harmful aftereffects is prevention by regular blood pressure (BP) measurements [1]. In order to avoid cases of masked HT in cuff-based measurements, the so far golden standard of HT detection, continuous BP monitoring methods are constantly developed [1]. Electrocardiography (ECG) and photoplethysmography (PPG) technologies are often recruited for this purpose [2–4]. Nevertheless, they are typically used in conjunction, which is not often feasible [2,3].

One of the most reliable methods which allows the BP estimation using only one of the aforementioned signal types is through heart-rate (HR) variability (HRV) analysis [5]. HRV is associated with BP through the autonomous nervous system (ANS)-baroreceptor connection [5]. A more specialized HRV analysis is HR asymmetry (HRA) analysis, which allows the separate investigation of the ANS components [6]. Curiously enough, HRA has not yet been recruited for BP-related research.

Traditionally, HRV is assessed from ECGs [4]. However, ECG technology is designed to be used for some hours or days, but not for longer use due to lack of comfort. A HRV equivalent could be PRV, derived likewise from PPGs. In this respect, only few studies have derived BP-related information from the HRV of PPGs [7–9].

The main reasons why PRV is not extensively utilized are trust issues posed often regarding the ability of PRV to resemble HRV and hence to extract BP-related information [10]. This fact significantly limits the progress in HT detection, as PPG technology is widely available and its use is imperceptible for the user. The present work aims to a deeper analysis of the PRV-HRV resemblance in BP monitoring and the development of optimized models based on PRV and PRA in order to efficiently detect HT.

2. Materials and Methods

The MIMIC database was used [11]. 202 ECG (lead II), PPG and ABP recordings with a duration of five minutes were extracted with an original sampling frequency of 125 Hz. ECGs were then resampled to 500 Hz and PPGs to 250 Hz to comply with the minimum sampling frequency recommendations for HRV/PRV calculation. ABP signals were exclusively used to manually classify the patients into one of the three BP categories: normotension (NT) (SBP<120 mmHg), prehypertension (PHT) (120 mmHg≤SBP<140 mmHg) and HT (SBP≥140 mmHg), where SBP is the systolic BP.

Preprocessing consisted of powerline interference, muscle noise, baseline wander and ectopics correction and R-peak detection for the ECGs [12–14]. Preprocessing for the PPG signals started with a high-pass Butterworth filter (2nd order) with a 0.5 Hz cut-off frequency and a 3-level discrete wavelet transform to remove the baseline fluctuation and the high frequency noise, preserving at the maximum the original signal's morphology. If present, ectopic beats were also corrected as with ECG. The final preprocessing step of the PPG signals was the detection of the PPG pulse peak, with a second derivative technique [15].

The HRV/PRV [5, 16] and HRA/PRA features were calculated [6], with the same technique for the ECGs and the PPGs, using the R and the pulse peaks, respectively. A list of the HRV/PRV and HRA/PRA features can be seen in Table 1. While each HRV/PRV feature reveals sympathetic or parasympathetic response, HRA/PRA can reveal either functions depending on its value.

For the statistical analysis, three separate groups were tested. In the first case, a 3-class split by NT, PHT and HT was performed (Group 3CL). In the second and third cases, binary splits were conducted (Groups NT/non-NT and HT/non-HT). Comparison at each group was performed by non-parametric tests (Kruskal-Wallis-KW for comparison among 3CL and Mann-Whitney U-test -MWU for each pair). Classification models were created by optimizable SVM classification with 10-fold cross validation and a test set of 20%, after feature selection with the help

Table 1. A list of the HRV/PRV and HRA/PRA features. HRA/PRA can be connected either with sympathetic or parasympathetic nervous system, depending on their score.

	Features	Details	
HRV/PRV	SDNN [ms]	sympathovagal balance	Response
	VARNN [ms]	sympathovagal balance	
	RMSSD [ms]	parasympathetic	
	pNN50 [ms]	parasympathetic	
	VLF [ms^2/Hz]	sympathetic	
	LF [ms^2/Hz]	sympathovagal/sympathetic	
	HF [ms^2/Hz]	parasympathetic	
	LF/HF	sympathovagal balance	
	SD1 [ms]	parasympathetic	
	SD2 [ms]	sympathovagal balance	
	SD1/SD2	sympathetic	
HRA/PRA	PI [6]	Porta's index	Full name
	GI [6]	Guzik's index	
	SI [6]	Slope index	
	AI [6]	Area index	
	DI	Deceleration index	

of ANOVA. Prior to feature selection, each feature was normalized according to their z-score to account for differences in magnitude due to different metrics.

For the HRV-PRV resemblance and differences in HT detection, Pearson correlation and Friedman ranksum (FR) tests were applied. Finally, the mean HRV/PRV differences were tested with Bland-Altman (BA).

3. Results

Table 2 shows the statistical comparison for each group. Due to lack of space, the PRA features that did not show statistically significant differences are omitted. For the 3CL group, all features vary significantly ($p < 0.05$) among the 3 BP states. The discrepancies are mainly found between PHT and HT classes. Regarding the NT-PHT comparison, statistically significant differences are only observed for pNN50 and PI, GI. In NT/non-NT group, statistically significant differences are detected in all PRV and PRA features but RMSSD, SD1 and LF/HF. For the HT/non-HT group, the only features that did not show a statistically significant difference were pNN50 and GI.

The accuracy of the best performing features as well as for the multi-feature classification is illustrated in Figure 1. For the 3CL group, the accuracy is shown by using once each class as positive. It can be easily observed that the 3CL group achieved the best accuracy for all features, although with small difference in most cases. Regarding the 1-vs-all analysis, the NT/non-NT group showed slightly better results in the single-feature classification but lower accuracy in the multi-feature classification (MC).

Overall, the MC showed the best results, with an accuracy of up to 95% for the 3CL, 90% for the NT/non-NT and 92.5% for the HT/non-HT, with models consisting of 6, 7 and 5 features, respectively. More specifically, SDNN, VARNN, pNN50, HF, SD1 and PI features were included in the model for the 3CL group, median, SDNN, VLF, SD2, SD1/SD2, PI and GI for the NT/non-NT and mean, RMSSD, VLF, LF and SD2 for the HT/non-HT model.

The resemblance study results can be seen in Table 3. Starting with correlation analysis (ρ), the results depend on the class type and the feature, with the HT class showing significantly higher correlations in most cases. Regarding the features, the highest correlations were observed for VLF, LF and SD2 in all BP types ($0.87-0.99$), with SDNN and VARNN showing also very high correlations for the PHT and HT classes. On the other hand, the lowest correlations were observed for RMSSD and LF/HF for all BP types ($0.22 - 0.99$), but more specifically for the NT type, where HF correlation was also quite low (0.22).

According to FR, HRV and PRV features were statistically different ($p \leq 0.001$). The percentage of recordings falling within the confidence interval (CI) indicates whether there is coherence between HRV/PRV. Indeed,

Table 2. Statistical comparison (KW and MWU) for the 3CL (first 4 columns) and the NT/non-NT and HT/non-HT groups.

Features	KW	NT-PHT	PHT-HT	NT-HT	NT/non-NT	HT/non-HT
SDNN	< 0.0001	0.0991	< 0.0001	0.0002	0.0431	< 0.0001
VARNN	< 0.0001	0.0991	< 0.0001	0.0002	0.0431	< 0.0001
RMSSD	0.0005	1.0000	0.0001	0.0099	0.0981	0.0002
pNN50	< 0.0001	0.0055	< 0.0001	0.0261	0.0001	0.9773
VLF	< 0.0001	0.1624	< 0.0001	0.0005	0.0327	< 0.0001
LF	< 0.0001	0.1166	< 0.0001	0.0001	0.0234	< 0.0001
HF	0.0001	0.6937	0.0001	0.0013	0.0187	< 0.0001
LF/HF	0.0051	0.0504	0.0011	0.3915	0.8898	0.0009
SD1	0.0005	1.0000	0.0001	0.0099	0.0981	0.0002
SD2	< 0.0001	0.2230	< 0.0001	0.0001	0.0149	< 0.0001
SD1/SD2	0.0146	0.6095	0.0035	0.0841	0.0431	< 0.0001
GI	< 0.0001	< 0.0001	0.0001	0.2089	0.0025	0.0709
PI	< 0.0001	< 0.0001	< 0.0001	0.1824	< 0.0001	0.0001

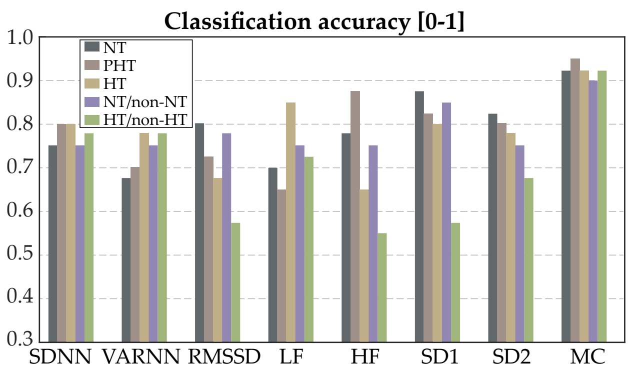

Figure 1. Classification accuracy for selected PRV features as well as the multi-feature classification (MC).

90% or more of the recordings were within CI, indicating high agreement. The same observation was corroborated by the BA ration (BAR), which depicts the ration of bias. In most cases, BAR was close to 0%, indicating a very high concordance, especially for frequency-domain features. SD1/SD2 showed values between $21 - 49\%$, indicating moderate to low agreement. LF/HF showed total incoherence, with very high BAR values.

4. Discussion

PRV-oriented study has potential in HT detection, but is often hindered due to dubious resemblance of PRV with HRV [10]. This study aimed to elucidate this issue by performing an exhaustive analysis on PRV-HRV correlation, including the assessment of discrepancies and similarities. Correlation and statistical comparison results were inconsistent, with correlations varying according to features and BP states, but showing generally satisfactory values, while FR indicating totally statistically significant differences. This incoherence highlights the importance of choosing the correct test depending on the analysis. The most suitable measure of similarity in biomedical data comparison is thought to be BA, which focuses on the mean difference between signals. As a matter of fact, BA analysis showed an overall high aptness of PRV to resemble HRV.

The second objective was to introduce implementable, optimized models able to detect HT or high BP from PPG recordings. 5- to 7-feature models were created using PRV and PRA features, achieving an accuracy of up to 95%, which is the highest reported so far in PRV-oriented studies [7–9]. The difference between the present and previous studies is the use of optimizable models, which are easy to be calculated as well as the inclusion of PRA, which offers a more profound insight of the autonomous nervous system function and hence a more complete BP-related analysis. The proposed models are rather simple, using only a few features. Therefore, they can be implemented in PPG technologies and contribute to the race against HT.

5. Conclusions

Although not in total agreement, PRV is a reliable HRV substitute in BP-oriented studies. The present work introduced simple, robust and reproducible models using PRV and PRA features able to detect HT. Given the high availability of PPG over ECG recordings, the use of these models could lead to a faster and more extensive HT detection.

Acknowledgments

Funding grants PID2021-00X128525-IV0 and PID2021-123804OB-I00 from Spanish Government and European Regional Development Fund (10.13039/501100011033), SBPLY/17/180501/000411 from Junta de Castilla-La Mancha and AICO/2021/286 from Generalitat Valenciana.

Table 3. Correlation (ρ), Friedman ranksum test (Fd) and Bland-Altman analysis (CI, BAR). Correlation ranges from $0-1$.

	NT				PHT				HT			
Feat.	ρ	**Fd** p	**CI** [%]	**BAR** [%]	ρ	**Fd** p	**CI** [%]	**BAR** [%]	ρ	**Fd** p	**CI** [%]	**BAR** [%]
SDNN	0.65	< 0.001	100	2.3	0.94	< 0.001	98	1.7	0.97	< 0.001	90	1.2
VARNN	0.55	< 0.001	100	0.2	0.98	< 0.001	93	0.2	0.99	< 0.001	97	0.1
RMSSD	0.30	< 0.001	96	1.7	0.72	< 0.001	95	1.5	0.87	< 0.001	97	1.9
VLF	0.95	< 0.001	92	0.4	0.98	< 0.001	98	1.1	0.97	< 0.001	98	0.1
LF	0.87	< 0.001	98	0.6	0.99	0.001	98	1.1	0.97	0.001	93	0.1
HF	0.22	< 0.001	96	0.3	0.50	< 0.001	98	1.4	0.99	< 0.001	98	0.1
LF/HF	0.57	< 0.001	92	717	0.23	< 0.001	91	360	0.68	< 0.001	97	207
SD1	0.30	< 0.001	96	2.4	0.72	< 0.001	95	2.1	0.87	< 0.001	97	2.7
SD2	0.87	< 0.001	98	1.8	0.97	< 0.001	98	1.5	0.99	< 0.001	94	0.7
SD1/ SD2	0.70	< 0.001	96	28	0.76	< 0.001	91	21	0.51	< 0.001	97	49

References

[1] Visseren FLJ, Mach F, Smulders YM, Carballo D, et al. 2021 ESC guidelines on cardiovascular disease prevention in clinical practice. European heart journal September 2021;42:3227–3337. ISSN 1522-9645.

[2] Allen J. Photoplethysmography and its application in clinical physiological measurement. Physiological measurement March 2007;28:R1–39. ISSN 0967-3334.

[3] Manga S, Muthavarapu N, Redij R, et al. Estimation of physiologic pressures: Invasive and non-invasive techniques, ai models, and future perspectives. Sensors Basel Switzerland June 2023;23. ISSN 1424-8220.

[4] Bird K, Chan G, et al. Assessment of hypertension using clinical electrocardiogram features: A first-ever review. Frontiers in medicine 2020;7:583331. ISSN 2296-858X.

[5] Yugar LBT, Yugar-Toledo JC, Dinamarco N, Sedenho-Prado LG, et al. The role of heart rate variability (HRV) in different hypertensive syndromes. Diagnostics Basel Switzerland February 2023;13. ISSN 2075-4418.

[6] Yan C, Li P, Li Y, Li J, Liu C. Analysis of heart rate asymmetry during sleep stages. ISSN 0922-6389, 2021; .

[7] Lan KC, Raknim P, Kao WF, Huang JH. Toward hypertension prediction based on ppg-derived hrv signals: a feasibility study. Journal of medical systems April 2018;42:103. ISSN 1573-689X.

[8] Octaviani A, Nuryani N, Salamah U, Utomo TP. Heart rate variability of photoplethysmography for hypertension detection using support vector machine. ISSN 1876-1100, 2023; 463–473.

[9] Mejía-Mejía E, May JM, Elgendi M, Kyriacou PA. Classification of blood pressure in critically ill patients using photoplethysmography and machine learning. Computer methods and programs in biomedicine September 2021; 208:106222. ISSN 1872-7565.

[10] Schäfer A, Vagedes J. How accurate is pulse rate variability as an estimate of heart rate variability? a review on studies comparing photoplethysmographic technology with an electrocardiogram. International journal of cardiology June 2013;166:15–29. ISSN 1874-1754.

[11] Goldberger AL, Amaral LA, Glass L, Hausdorff JM, Ivanov PC, Mark RG, Mietus JE, Moody GB, Peng CK, Stanley HE. Physiobank, physiotoolkit, and physionet: components of a new research resource for complex physiologic signals. Circulation June 2000;101:E215–E220. ISSN 1524-4539.

[12] García M, Martínez-Iniesta M, Ródenas J, Rieta JJ, Alcaraz R. A novel wavelet-based filtering strategy to remove powerline interference from electrocardiograms with atrial fibrillation. Physiological measurement November 2018; 39:115006. ISSN 1361-6579.

[13] Sörnmo L, Laguna P. Electrocardiogram (ECG) Signal Processing, volume 2. United States: John Wiley and Sons. ISBN 978-0-471-24967-2 (set), 2006; 1298–1313.

[14] Martínez A, Alcaraz R, Rieta JJ. Application of the phasor transform for automatic delineation of single-lead ECG fiducial points. Physiol Meas Nov 2010;31(11):1467–85.

[15] Anisimov A, Alekseev B, Egorov D. Comparison of heart rate derived from ECG and pulse wave signals during controlled breathing test for biofeedback systems. In 2021 IEEE Ural-Siberian Conference on Computational Technologies in Cognitive Science, Genomics and Biomedicine (CSGB). 2021; 430–434.

[16] Heart rate variability. standards of measurement, physiological interpretation, and clinical use. task force of the european society of cardiology and the north american society of pacing and electrophysiology. European heart journal March 1996;17:354–381. ISSN 0195-668X.

Address for correspondence:

José J. Rieta
BioMIT.org, Electronic Engineering Department, Building 7F, Universitat Politecnica de Valencia, 46022 Valencia, Spain.
e-mail: jjrieta@upv.es